Creation of Ultracold Sr_2 Molecules in the Electronic Ground State

Simon Stellmer,[1] Benjamin Pasquiou,[1] Rudolf Grimm,[1,2] and Florian Schreck[1]

[1] *Institut für Quantenoptik und Quanteninformation (IQOQI), Österreichische Akademie der Wissenschaften, 6020 Innsbruck, Austria*

[2] *Institut für Experimentalphysik und Zentrum für Quantenphysik, Universität Innsbruck, 6020 Innsbruck, Austria*

(Received 20 May 2012; published 13 September 2012)

We report on the creation of ultracold $^{84}Sr_2$ molecules in the electronic ground state. The molecules are formed from atom pairs on sites of an optical lattice using stimulated Raman adiabatic passage (STIRAP). We achieve a transfer efficiency of 30% and obtain 4×10^4 molecules with full control over the external and internal quantum state. STIRAP is performed near the narrow $^1S_0$-$^3P_1$ intercombination transition, using a vibrational level of the $1(0_u^+)$ potential as an intermediate state. In preparation of our molecule association scheme, we have determined the binding energies of the last vibrational levels of the $1(0_u^+)$, $1(1_u)$ excited-state and the $X\,^1\Sigma_g^+$ ground-state potentials. Our work overcomes the previous limitation of STIRAP schemes to systems with magnetic Feshbach resonances, thereby establishing a route that is applicable to many systems beyond alkali-metal dimers.

DOI: 10.1103/PhysRevLett.109.115302 PACS numbers: 67.85.−d, 03.75.Nt, 34.50.Rk, 37.10.Pq

The creation of ultracold molecular gases has made rapid progress over the past years. The rich internal structure of molecules combined with low translational energy enables precision measurements of fundamental constants, realizations of novel quantum phases, and applications for quantum computation [1]. A very successful route to large samples of ultracold molecules with complete control over the internal and external quantum state is association of molecules from ultracold atoms. Early experiments used magnetic Feshbach resonances to form weakly bound alkali-metal molecules, some of which have even been cooled to quantum degeneracy [2]. Stimulated Raman adiabatic passage (STIRAP) [3] has enabled the coherent transfer of these Feshbach molecules into the vibrational ground state [4–6]. In particular, heteronuclear molecules in the vibrational ground state have received a lot of attention, because they possess a strong electric dipole moment, leading to anisotropic, long-range dipole-dipole interactions, which will enable studies of fascinating many-body physics [7]. Efforts are underway to create samples of completely state-controlled molecules beyond alkali-metal dimers [8–10], which will widen the range of applications that can be reached experimentally.

So far, the key step in the efficient creation of ultracold molecules has been molecule association using magnetic Feshbach resonances. This magnetoassociation technique cannot be used to form dimers of alkaline-earth-metal atoms or ytterbium, because of the lack of magnetic Feshbach resonances in these nonmagnetic species. An example is Sr_2, which has been proposed as a sensitive and model-independent probe for time variations of the proton-to-electron mass ratio [11–13]. Another class of molecules for which magnetoassociation is difficult are dimers containing an alkali-metal atom and a nonmagnetic atom, since in these cases magnetic Feshbach resonances are extremely narrow [14,15]. This difficulty occurs in current experimental efforts to create LiYb, RbYb, or RbSr molecules [8–10]. Other molecule creation techniques that are suitable for dimers containing nonmagnetic atoms have been proposed. Examples are molecule formation by STIRAP from a Bose-Einstein condensate (BEC) [16–19] or from atom pairs in a deep optical lattice [20], as well as two-color photoassociation (PA) of atom pairs in a Mott insulator [21].

In this Letter, we show that ultracold Sr_2 molecules in the electronic ground state can be efficiently formed, despite the lack of a magnetic Feshbach resonance. Instead of magnetoassociation, we combine ideas from Refs. [16–21] and use optical transitions to transform pairs of atoms into molecules by STIRAP. The molecule conversion efficiency is enhanced by preparing pairs of atoms in a Mott insulator on the sites of an optical lattice [22,23]. We achieve an efficiency of 30% and create samples of 4×10^4 $^{84}Sr_2$ molecules. We perform PA spectroscopy to identify the vibrational levels and optical transitions used for molecule creation.

STIRAP coherently transfers an initial two-atom state $|a\rangle$ into a molecule $|m\rangle$ by optical transitions; see Fig. 1. In our case, the initial state $|a\rangle$ consists of two ^{84}Sr atoms occupying the ground state of an optical lattice well. The final state $|m\rangle$ is a Sr_2 molecule in the second-to-last ($\nu = -2$) vibrational level of the $X\,^1\Sigma_g^+$ ground-state molecular potential without rotational angular momentum. The molecules have a binding energy of 645 MHz and are also confined to the ground state of the lattice well. States $|a\rangle$ and $|m\rangle$ are coupled by laser fields L_1 and L_2, respectively, to state $|e\rangle$, the third-to-last ($\nu' = -3$) vibrational level of the metastable $1(0_u^+)$ state, dissociating to $^1S_0$-$^3P_1$.

We use the isotope ^{84}Sr for molecule creation, since it is ideally suited for the creation of a BEC [24,25] and formation of a Mott insulator. The binding energies of the vibrational levels involved in our STIRAP scheme are

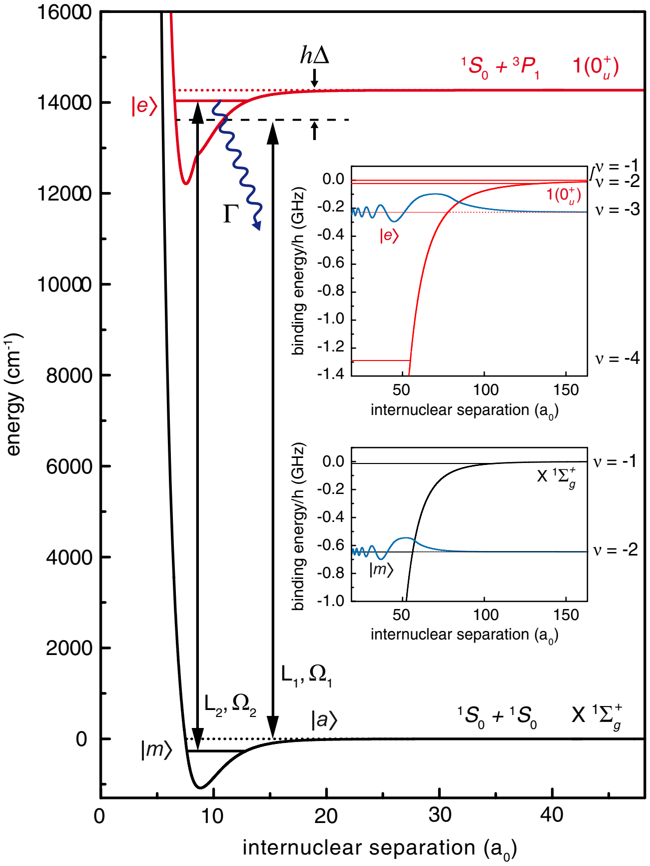

FIG. 1 (color online). Molecular potentials and vibrational levels of ^{84}Sr$_2$ involved in STIRAP. The initial state $|a\rangle$, an atom pair in the ground state of an optical lattice well, and the final molecular state $|m\rangle$ are coupled by laser fields L_1 and L_2 to the excited state $|e\rangle$ with Rabi frequencies Ω_1 and Ω_2, respectively. The parameter Δ is the detuning of L_1 from the ${}^1S_0$-${}^3P_1$ transition, and Γ is the decay rate of $|e\rangle$. The insets show the last vibrational levels of the molecular potentials and the wave functions of states $|m\rangle$ and $|e\rangle$. For comparison, the wave function of atomic state $|a\rangle$ (not shown) has its classical turning point at a radius of $800a_0$, where a_0 is the Bohr radius. The potentials are taken from Refs. [39,40], and the wave functions are calculated by using the WKB approximation. The energies of states $|m\rangle$ and $|e\rangle$ are not to scale in the main figure.

known only for the isotope ^{88}Sr [26,27] and can be estimated for ^{84}Sr by mass scaling [28,29]. An essential task in preparation for molecule creation is therefore to spectroscopically determine the binding energies of relevant ^{84}Sr$_2$ levels.

We perform PA spectroscopy [30] on a ^{84}Sr BEC, produced similarly to our previous work [24]. The BEC is confined in an oblate crossed-beam optical dipole trap with oscillation frequencies of 55 Hz in the horizontal plane and 180 Hz in the vertical direction, based on two 5-W laser sources operating at 1064 nm with a linewidth of 3 nm. Laser fields L_1 and L_2, which are used for spectroscopy and STIRAP, have linewidths of ~2 kHz and are referenced with an accuracy better than 1 kHz to the ${}^1S_0$-${}^3P_1$ intercombination line, which has a natural width of $\Gamma/2\pi = 7.4$ kHz. To achieve the coherence of the laser fields required for STIRAP, L_1 and L_2 are derived from the same master laser by means of acousto-optical modulators. These laser beams are copropagating in the same spatial mode with a waist of 100(25) μm on the atoms and are linearly polarized parallel to a guiding magnetic field of 120 mG.

One-color PA spectroscopy is used to determine the binding energies of the last four vibrational levels of the $1(0_u^+)$ state. To record the loss spectrum, we illuminate the BEC for 100 ms with L_1 for different detunings Δ with respect to the ${}^1S_0$-${}^3P_1$ transition. The binding energies derived from these measurements are presented in Table I.

We then use two-color PA spectroscopy to determine the binding energies of the last vibrational levels of the $X\,{}^1\Sigma_g^+$ ground-state potential. The loss spectra are recorded in the same manner as for one-color PA spectroscopy, just with the additional presence of L_2. Figure 2 shows two spectra, for which L_2 is on resonance with the transition from state $|m\rangle$ to state $|e\rangle$. The difference between the spectra is the intensity of L_2. The spectrum shown in Fig. 2(a) was recorded at high intensity and displays an Autler-Townes splitting [31]. In this situation, the coupling of states $|m\rangle$ and $|e\rangle$ by L_2 leads to a doublet of dressed states, which is probed by L_1. The data of Fig. 2(b) were recorded at low intensity and show a narrow dark resonance at the center of the PA line. Here, a superposition of states $|a\rangle$ and $|m\rangle$ is formed, for which the amplitudes of excitation by L_1 and L_2 destructively interfere. The binding energies of the ground-state vibrational levels derived from measurements of dark resonances are given in Table I.

The Rabi frequencies $\Omega_{1,2}$ of our coupling lasers are determined by fitting a three-mode model to the spectra [32]; see Fig. 2. The free-bound Rabi frequency Ω_1 scales with intensity I_1 of L_1 and atom density ρ as $\Omega_1 \propto \sqrt{I_1}\sqrt{\rho}$ [17]. The bound-bound Rabi frequency $\Omega_2 \propto \sqrt{I_2}$ depends only on the intensity I_2 of L_2. We obtain $\Omega_1/(\sqrt{I_1}\sqrt{\rho/\rho_0}) = 2\pi \times 10(4)\ \text{kHz}/\sqrt{\text{W/cm}^2}$ at a peak density of $\rho_0 = 4\times 10^{14}\ \text{cm}^{-3}$ and $\Omega_2/\sqrt{I_2} = 2\pi\times 50(15)\ \text{kHz}/\sqrt{\text{W/cm}^2}$, where the error is dominated by uncertainty in the laser beam intensity.

TABLE I. Binding energies of the highest vibrational levels of the $1(0_u^+)$, $1(1_u)$, and $X\,{}^1\Sigma_g^+$ $(l = 0, 2)$ states, where l is the rotational angular momentum quantum number. The levels are labeled by ν, starting from above with $\nu = -1$. Measurement procedure and error discussion are given in Ref. [30].

ν	$1(0_u^+)$ (MHz)	$1(1_u)$ (MHz)	$X\,{}^1\Sigma_g^+(l=0)$ (MHz)	$X\,{}^1\Sigma_g^+(l=2)$ (MHz)
−1	−0.32(1)	−351.45(2)	−13.7162(2)	⋯
−2	−23.01(1)		−644.7372(2)	−519.6177(5)
−3	−228.38(1)			
−4	−1288.29(1)			

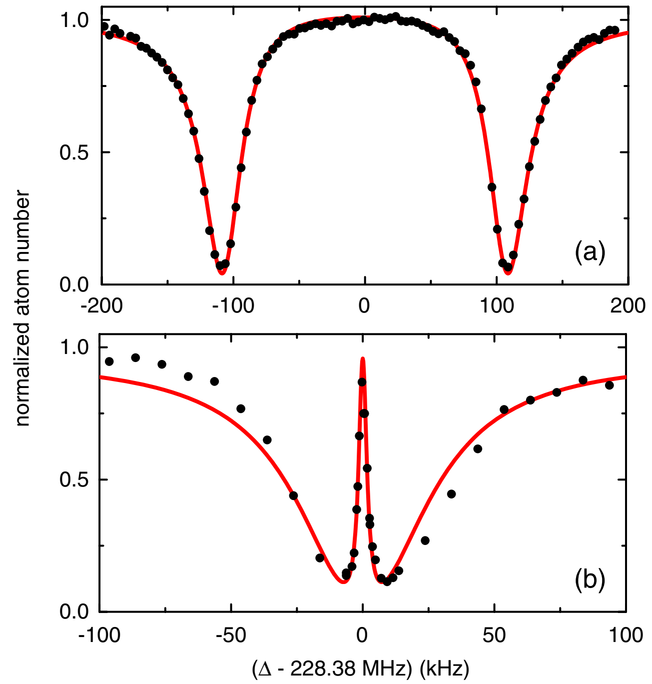

FIG. 2 (color online). Two-color PA spectra near state $|e\rangle$ for two intensities of L_2. (a) For high intensity (20 $\mathrm{W/cm^2}$) the spectrum shows an Autler-Townes splitting. (b) For low intensity (80 $\mathrm{mW/cm^2}$) a narrow dark resonance is visible. For both spectra, the sample was illuminated by L_1 for 100 ms with an intensity of 7 $\mathrm{mW/cm^2}$ at varying detuning Δ from the ${}^1S_0$-${}^3P_1$ transition. The lines are fits according to a three-mode model [32].

To enhance molecule formation, we create a Mott insulator by loading the BEC into an optical lattice [33]. The local density increase on a lattice site leads to an increased free-bound Rabi frequency Ω_1. Furthermore, molecules are localized on lattice sites and thereby protected from inelastic collisions with each other. The lattice is formed by three nearly orthogonal retroreflected laser beams with waists of 100 μm on the atoms, derived from an 18-W single-mode laser operating at a wavelength of $\lambda = 532$ nm. Converting the BEC into a Mott insulator is done by increasing the lattice depth during 100 ms to $16.5E_{\mathrm{rec}}$, where $E_{\mathrm{rec}} = \hbar^2k^2/2m$ is the recoil energy with $k = 2\pi/\lambda$ and m the mass of a strontium atom. After lattice ramp-up, the 1064-nm dipole trap is ramped off in 100 ms.

To estimate the number of doubly occupied sites, which are the sites relevant for molecule formation, we analyze the decay of the lattice gas under different conditions. After loading a BEC with less than $\sim 3 \times 10^5$ atoms into the lattice, the lifetime of the lattice gas is 10(1) s. For higher BEC atom numbers, we observe an additional, much faster initial decay on a time scale of 50 ms, which removes a fraction of the atoms. We attribute this loss to three-body decay of triply occupied sites, which are formed only if the BEC peak density is high enough. To obtain a high number of doubly occupied sites, we load a large BEC of 1.5×10^6 atoms into the lattice. After the initial decay, 6×10^5 atoms remain. By inducing PA loss using L_1, we can show that half of these atoms occupy sites in pairs.

We are now ready to convert the atom pairs on doubly occupied sites into molecules by STIRAP. This method relies on a counterintuitive pulse sequence [3], during which L_2 is pulsed on before L_1. During this sequence, the atoms populate the dark state $|\Psi\rangle = (\Omega_1|m\rangle + \Omega_2|a\rangle)/(\Omega_1^2 + \Omega_2^2)^{1/2}$, where Ω_1 and Ω_2 are the time-dependent Rabi frequencies of the two coupling laser fields as defined in Ref. [3], which can reach up to $\Omega_1^{\max} \sim 2\pi \times 150$ kHz and $\Omega_2^{\max} = 2\pi \times 170(10)$ kHz in our case [34]. Initially, the atoms are in state $|a\rangle$, which is the dark state after L_2 is suddenly switched on but L_1 kept off. During the pulse sequence, which takes $T = 100$ μs, L_1 is ramped on and L_2 off; see association STIRAP in Fig. 3(a). This adiabatically evolves the dark state into $|m\rangle$ if $\Omega_{1,2}^{\max} \gg 1/T$, a condition which we fulfill. To end the pulse sequence, L_1 is suddenly switched off. During the whole process, state $|e\rangle$ is only weakly populated, which avoids loss of atoms by spontaneous emission if $\Omega_{1,2}^{\max} \gg \Gamma$. This condition is easily fulfilled with a narrow transition such as

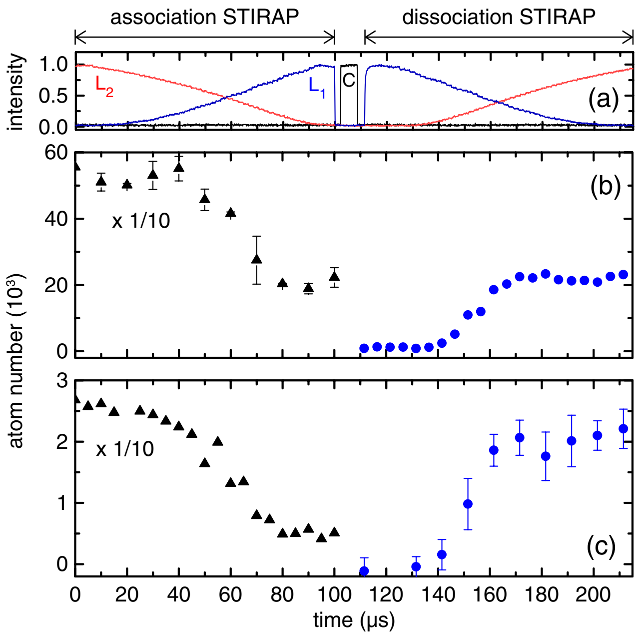

FIG. 3 (color online). Time evolution of STIRAP transfers from atom pairs to $\mathrm{Sr_2}$ molecules and back. (a) Intensities of L_1, L_2, and cleaning laser C, normalized to one. (b),(c) Atom number evolution. For these measurements, L_1 and L_2 are abruptly switched off at a given point in time, and the atom number is recorded on an absorption image after 10 ms free expansion. Note the scaling applied to data taken during the first 100 μs (triangles). The starting point for the time evolution shown in (b) is a Mott insulator, whereas the starting point for (c) is a sample for which 80% of the atoms occupy lattice sites in pairs.

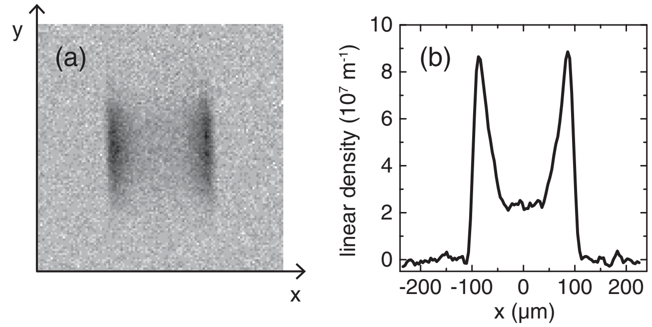

FIG. 4. Quasimomentum distribution of repulsively bound pairs. (a) Average of 20 absorption images recorded 10 ms after release of the atoms from the lattice. (b) Integral of the distribution along y.

the one used here. The association STIRAP transfer does not lead to molecules in excited lattice bands, since T is long enough for the band structure to be spectrally resolved.

We now characterize the molecule creation process. To detect molecules, we dissociate them by using a time-mirrored pulse sequence [dissociation STIRAP in Fig. 3(a)] and take absorption images of the resulting atoms. The atom number evolution during molecule association and dissociation is shown in Fig. 3(b). After the molecule association pulse sequence, 2×10^5 atoms remain, which we selectively remove by a pulse of light resonant to the ${}^1S_0$-${}^1P_1$ atomic transition, out of resonance with any molecular transition [36]; see "cleaning" laser C in Fig. 3(a). The recovery of 2×10^4 atoms by the dissociation STIRAP confirms that molecules have been formed. Further evidence that molecules are the origin of recovered atoms is that 80% of these atoms occupy lattice sites in pairs. Quantitatively, this is shown by removing atom pairs using PA and measuring the loss of atoms. Qualitatively, we illustrate this fact by creating and detecting one-dimensional repulsively bound pairs along the x direction [37]. The pairs were created by ramping the x-direction lattice beam to a value of $10E_{\mathrm{rec}}$ before ramping all lattice beams off, which propels the pairs into free atoms with opposite momenta along x. Figure 4 shows the characteristic momentum space distribution of these pairs.

To estimate the STIRAP efficiency and subsequently the number of molecules, we perform another round of molecule association and dissociation on such a sample of atoms with large fraction of doubly occupied sites; see Fig. 3(c). We recover $f = 9\%$ of the atoms, which corresponds to a single-pass efficiency of $\sqrt{f} = 30\%$. The largest sample of atoms created by dissociating molecules contains $N_a = 2.5 \times 10^4$ atoms, which corresponds to $N_m = N_a/(2\sqrt{f}) = 4 \times 10^4$ molecules.

We measure the lifetime of molecules in the lattice, by varying the hold time between molecule creation and dissociation. We obtain ~60 μs, nearly independent of the lattice depth. Executing the cleaning laser pulse after the hold time instead of before does not change the lifetime. This time is surprisingly short and can be explained neither by scattering of lattice photons nor by tunneling of atoms or molecules confined to the lowest band of the lattice and subsequent inelastic collisions. By band mapping [38], we observe that 3×10^4 of the initial 6×10^5 atoms are excited to the second band during the association STIRAP, and more atoms have possibly been excited to even higher bands. We speculate that these atoms, which move easily through the lattice, collide inelastically with the molecules, resulting in the observed short molecule lifetime. The cleaning laser pulse is not able to push these atoms out of the region of the molecules fast enough to avoid the loss. The short lifetime can explain the 30% limit of the molecule conversion efficiency. Without the loss, the high Rabi frequencies and the good coherence of the coupling lasers should result in a conversion efficiency close to 100%. The excitation of atoms to higher bands cannot be explained by off-resonant excitation of atoms by L_1 or L_2. Incoherent light of the diode lasers on resonance with the atomic transition might be the reason for the excitation. Further investigation of the excitation mechanism is needed in order to circumvent it.

In conclusion, we have demonstrated that it is possible to use STIRAP to coherently create Sr_2 molecules from atom pairs on the sites of an optical lattice. The advantage of this technique compared to the traditional magnetoassociation approach is that it can be used for systems that do not possess a suitable magnetic Feshbach resonance. This new approach might be essential for the formation of dimers containing an alkali-metal atom and a nonmagnetic atom, such as RbSr.

We thank Manfred Mark for helpful discussions. We gratefully acknowledge support from the Austrian Ministry of Science and Research (BMWF) and the Austrian Science Fund (FWF) through a START grant under Project No. Y507-N20. As a member of the project iSense, we also acknowledge financial support of the Future and Emerging Technologies (FET) program within the Seventh Framework Programme for Research of the European Commission, under FET-Open Grant No. 250072.

---

[1] *Cold Molecules: Theory, Experiment, Applications*, edited by R. V. Krems, B. Friedrich, and W. C. Stwalley (Taylor & Francis, London, 2009).
[2] F. Ferlaino, S. Knoop, and R. Grimm, in Ref. [1], Chap. 9.
[3] N. V. Vitanov, T. Halfmann, B. W. Shore, and K. Bergmann, Annu. Rev. Phys. Chem. **52**, 763 (2001).
[4] J. G. Danzl, E. Haller, M. Gustavsson, M. J. Mark, R. Hart, N. Bouloufa, O. Dulieu, H. Ritsch, and H.-C. Nägerl, Science **321**, 1062 (2008).
[5] F. Lang, K. Winkler, C. Strauss, R. Grimm, and J. Hecker Denschlag, Phys. Rev. Lett. **101**, 133005 (2008).
[6] K.-K. Ni, S. Ospelkaus, M. H. G. de Miranda, A. Pe'er, B. Neyenhuis, J. J. Zirbel, S. Kotochigova, P. S. Julienne, D. S. Jin, and J. Ye, Science **322**, 231 (2008).

[7] G. Pupillo, A. Micheli, H. P. Büchler, and P. Zoller, in Ref. [1], Chap. 12.

[8] H. Hara, Y. Takasu, Y. Yamaoka, J. M. Doyle, and Y. Takahashi, Phys. Rev. Lett. **106**, 205304 (2011).

[9] A. H. Hansen, A. Khramov, W. H. Dowd, A. O. Jamison, V. V. Ivanov, and S. Gupta, Phys. Rev. A **84**, 011606 (2011).

[10] N. Nemitz, F. Baumer, F. Münchow, S. Tassy, and A. Görlitz, Phys. Rev. A **79**, 061403 (2009).

[11] T. Zelevinsky, S. Kotochigova, and J. Ye, Phys. Rev. Lett. **100**, 043201 (2008).

[12] S. Kotochigova, T. Zelevinsky, and J. Ye, Phys. Rev. A **79**, 012504 (2009).

[13] K. Beloy, A. W. Hauser, A. Borschevsky, V. V. Flambaum, and P. Schwerdtfeger, Phys. Rev. A **84**, 062114 (2011).

[14] P. S. Zuchowski, J. Aldegunde, and J. M. Hutson, Phys. Rev. Lett. **105**, 153201 (2010).

[15] D. A. Brue and J. M. Hutson, Phys. Rev. Lett. **108**, 043201 (2012).

[16] M. Mackie, R. Kowalski, and J. Javanainen, Phys. Rev. Lett. **84**, 3803 (2000).

[17] P. D. Drummond, K. V. Kheruntsyan, D. J. Heinzen, and R. H. Wynar, Phys. Rev. A **65**, 063619 (2002).

[18] M. Mackie, A. Collin, and J. Javanainen, Phys. Rev. A **71**, 017601 (2005).

[19] P. D. Drummond, K. V. Kheruntsyan, D. J. Heinzen, and R. H. Wynar, Phys. Rev. A **71**, 017602 (2005).

[20] M. Tomza, F. Pawłowski, M. Jeziorska, C. P. Koch, and R. Moszynski, Phys. Chem. Chem. Phys. **13**, 18 893 (2011).

[21] D. Jaksch, V. Venturi, J. I. Cirac, C. J. Williams, and P. Zoller, Phys. Rev. Lett. **89**, 040402 (2002).

[22] D. Jaksch, C. Bruder, J. I. Cirac, C. W. Gardiner, and P. Zoller, Phys. Rev. Lett. **81**, 3108 (1998).

[23] M. Greiner, O. Mandel, T. Esslinger, T. W. Hänsch, and I. Bloch, Nature (London) **415**, 39 (2002).

[24] S. Stellmer, M. K. Tey, B. Huang, R. Grimm, and F. Schreck, Phys. Rev. Lett. **103**, 200401 (2009).

[25] Y. N. Martinez de Escobar, P. G. Mickelson, M. Yan, B. J. DeSalvo, S. B. Nagel, and T. C. Killian, Phys. Rev. Lett. **103**, 200402 (2009).

[26] T. Zelevinsky, M. M. Boyd, A. D. Ludlow, T. Ido, J. Ye, R. Ciuryło, P. Naidon, and P. S. Julienne, Phys. Rev. Lett. **96**, 203201 (2006).

[27] Y. N. Martinez de Escobar, P. G. Mickelson, P. Pellegrini, S. B. Nagel, A. Traverso, M. Yan, R. Côté, and T. C. Killian, Phys. Rev. A **78**, 062708 (2008).

[28] G. F. Gribakin and V. V. Flambaum, Phys. Rev. A **48**, 546 (1993).

[29] B. Gao, Phys. Rev. A **62**, 050702 (2000).

[30] See Supplemental Material at http://link.aps.org/supplemental/10.1103/PhysRevLett.109.115302 for details
on the PA spectroscopy.

[31] S. H. Autler and C. H. Townes, Phys. Rev. **100**, 703 (1955).

[32] K. Winkler, G. Thalhammer, M. Theis, H. Ritsch, R. Grimm, and J. H. Denschlag, Phys. Rev. Lett. **95**, 063202 (2005).

[33] S. Stellmer, Ph.D. thesis, University of Innsbruck (unpublished).

[34] Note that Refs. [3,32,35] use different definitions of Ω_1, which we note here as Ω_1^{BEC} and Ω_1^{MI}. We use the three-mode model of Ref. [32] to determine Ω_1^{BEC} from two-color PA spectroscopy of a BEC. This model is not able to describe STIRAP starting from an atom pair on a lattice site. Suitable models are given in Refs. [3,35] and use Ω_1^{MI}, which we approximate by $\Omega_1^{\mathrm{MI}} \sim \sqrt{2}\sqrt{\rho_0^{\mathrm{MI}}/\rho_0^{\mathrm{BEC}}}\sqrt{I_1^{\mathrm{STIRAP}}/I_1^{\mathrm{PA}}}\,\Omega_1^{\mathrm{BEC}}$. Here $\rho_0^{\mathrm{BEC}} = 4 \times 10^{14}\ \mathrm{cm}^{-3}$ is the peak density of the BEC, $\rho_0^{\mathrm{MI}} = 5 \times 10^{15}\ \mathrm{cm}^{-3}$ the peak density of an atom pair on a lattice site, I_1^{PA} the intensity of L_1 used for PA spectroscopy, and I_1^{STIRAP} the intensity of L_1 used during STIRAP, which is maximally $10\ \mathrm{W/cm}^2$. The factor $\sqrt{2}$ is discussed in Ref. [19].

[35] K. Winkler, F. Lang, G. Thalhammer, P. van der Straten, R. Grimm, and J. Hecker Denschlag, Phys. Rev. Lett. **98**, 043201 (2007).

[36] The pulse of light (duration 7 μs, intensity 250 $\mathrm{mW/cm}^2$) separates the atoms in momentum space from the molecules, which leads to a spatial separation on absorption images recorded after 10 ms free expansion.

[37] K. Winkler, G. Thalhammer, F. Lang, R. Grimm, J. Hecker Denschlag, A. J. Daley, A. Kantian, H. P. Büchler, and P. Zoller, Nature (London) **441**, 853 (2006).

[38] M. Greiner, I. Bloch, O. Mandel, T. W. Hänsch, and T. Esslinger, Phys. Rev. Lett. **87**, 160405 (2001).

[39] A. Stein, H. Knöckel, and E. Tiemann, Phys. Rev. A **78**, 042508 (2008).

[40] W. Skomorowski, F. Pawlowski, C. P. Koch, and R. Moszynski, J. Chem. Phys. **136**, 194306 (2012).